communications physics

A Nature Portfolio journal

Article

https://doi.org/10.1038/s42005-025-02191-1

Topology in the random scattering of light

Tobias Micklitz [1] ✉ & Alexander Altland [2] ✉

Light scattering in random media is usually considered within the framework of the three-dimensional Anderson universality class, with modifications for the vector nature of electromagnetic waves. We propose that the linear dispersiveness of light introduces topological aspects into the picture. The dynamics of electromagnetic waves follow the same differential equations as those of a spin-1 Weyl semimetal. In the presence of disorder, this equivalence leads to a range of phenomena explored in this paper. These include topological protection against localization when helicity hybridization is weak, the emergence of exotic phases in weakly scattering media, and anomalies in optical transparency in the presence of synthetic 'magnetic fields'. We argue that some of these effects should be visible and investigated already in weakly disordered optical materials.

The propagation of light through disordered media gives rise to complex interference phenomena with a wide range of practical applications, from photocatalysis[1,2] and random lasing[3–5] to optical sensing[6]. Despite conceptual parallels to the physics of scalar waves in random media, the scattering of light remains partially enigmatic. One of the most intriguing theoretical predictions—three-dimensional Anderson localization of light under strong disorder—remains 'stubbornly elusive' and experimentally unobserved. This persistent absence has been attributed to the vectorial nature of light[7,8], distinguishing it from simpler scalar wave models where localization under strong disorder is well established[9–19].

Here, we demonstrate that random scattering of light exhibits a complementary mechanism beyond conventional Anderson localization: topologically driven anomalies rooted in helicity conservation. We show that light transport in random media can exhibit robust anomalies analogous to those in topological fermionic matter, when helicity—the projection of angular momentum along the direction of propagation—relaxes slowly. Our analysis relies on a formal mapping between Maxwell's equations and the Schrödinger equation of a spin-1 Weyl semimetal, a class of topological systems recently identified in fermionic band insulators with crystalline symmetries[20]. In this analogy, the transverse components of light correspond to spin-z projections ± 1, while longitudinal modes map to $s_z = 0$, and the Weyl cones represent left- and right-handed helicities. Both systems exhibit linear dispersion and a well-defined handedness, making helicity the classical analog of spin and a central symmetry of the problem.

In free space, the helicity of light is conserved. This symmetry is, however, typically broken in random optical media, where scattering mixes left- and right-handed circular polarizations. To anticipate classes of optical materials likely to exhibit helicity-protected transport phenomena, we recall that in random media, the local material parameters dielectric permittivity $\epsilon_{\mathbf{x}}$ and magnetic permeability $\mu_{\mathbf{x}}$ define the spatially varying refractive index and impedance,

$$n_{\mathbf{x}} = \sqrt{\mu_{\mathbf{x}}\epsilon_{\mathbf{x}}}, \qquad Z_{\mathbf{x}} = \sqrt{\mu_{\mathbf{x}}/\epsilon_{\mathbf{x}}}, \tag{1}$$

respectively. Media with constant impedance, where $\mu_{\mathbf{x}} \propto \epsilon_{\mathbf{x}}$, preserve electric-magnetic duality, much like the vacuum, and thus conserve helicity even in the presence of disorder (Fig. 1). Materials approaching this duality condition, such as sub-wavelength dielectric spheres[21,22] and high-index semiconductors, including silicon, germanium, and rutile-TiO_2[22], exhibit near-conservation of helicity over specific frequency ranges, as demonstrated by persistent circular polarization in scattering experiments. These systems realize what is known as the 'first Kerker condition'[23] and provide fertile ground for observing topology-driven transport phenomena in optics.

In generic disordered media, where helicity is not strictly conserved, these anomalies become fragile. Nevertheless, as long as helicity mixing remains weak, light propagation retains an anomalous character over intermediate length scales. A spectral flow mechanism[24,25], analogous to that in Weyl semimetals, continues to be at work, and raises key questions: how far do the anomalies extend, and what signatures do they leave in measurable optical observables? To address these questions, we develop an effective field theory of light transmission in disordered media that captures the physics beyond the scattering mean free path. The theory generalizes the Chern-Simons (CS) framework developed for spin-1/2 Weyl fermions[24,26] to spin-1 electromagnetic fields. It identifies two central parameters: a bare transmission coefficient σ, derived within a self-consistent Born approximation, and a golden rule helicity-mixing rate Γ_{h}, which quantifies coupling between opposite helicities. Together, these parameters define a nonlinear σ-model (cf. Eqs. (6) and Eqs. (8) below), generalizing the field theory of light pioneered by John[27–29] to individually resolved helical sectors. Crucially, each sector contributes a topological Chern-Simons term to the action (Eq. (7)),

[1]Centro Brasileiro de Pesquisas Físicas, Rua Xavier Sigaud 150, Rio de Janeiro, Brazil. [2]Institut für Theoretische Physik, Universität zu Köln, Zülpicher Str. 77, Cologne, Germany. ✉e-mail: tobias.micklitz@gmail.com; alexal@thp.uni-koeln.de

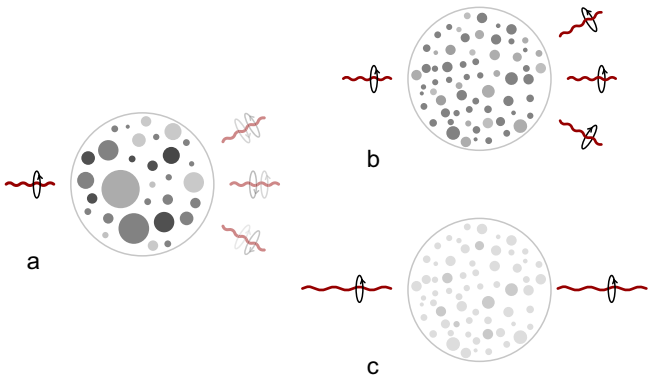

Fig. 1 | Helicity conserving media. a The scattering of light in generic optical media may alter its helicity, indicated by clock- or anticlockwise revolving circles. **b** In helicity-conserving media, such as synthetically engineered sub-wavelength dielectric spheres[21,22], a complete attenuation of transmitted signals by Anderson localization is blocked by topological principles. **c** Within this class of materials, there may exist a regime with low but non-vanishing scattering rates where media look effectively transparent in the large wavelength limit.

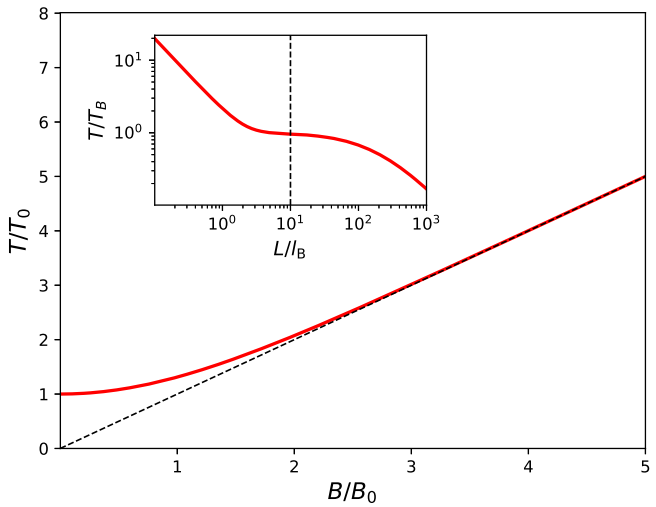

Fig. 2 | Transmission, *T*, vs. magnetic field *B*. Here $T_0 = R^2\sigma/(8L)$ and $B_0 = \sigma/(4L)$, and assuming $l_h > L$. For $B > B_0$ the field dependence becomes asymptotically linear. Inset: T vs. length L in units of l_B, with $l_h = 10 l_B$ (indicated by the vertical dashed line) and $T_B = R^2B/2$. For further details on the parameters, see the discussion below Eq. (8).

which enforces non-vanishing transmission and blocks localization. This anomaly persists up to a crossover length scale $l_h \sim \sqrt{\sigma/\Gamma_h}$, beyond which helicity mixing restores conventional, diffusive transport.

Building on Chern-Simons theory, we uncover three qualitatively distinct transport regimes, each governed by the level of disorder and the extent of helicity conservation. These include a topological suppression of Anderson localization, anomalous transport analogous to effects in Weyl semimetals, and a transition to an effectively transparent phase at weak disorder. Together, they reveal a class of phenomena inaccessible to scalar wave theories and underscore the need for a topology-aware framework—an approach we develop and apply in the following sections.

Results and discussion

We now examine the three disorder-dependent transport regimes in detail. Each reflects a unique topological response captured by the Chern-Simons theory framework, and each is missed by conventional scalar descriptions of light scattering.

Strong 'dual' disorder: absence of Anderson localization

Light scattering in the limiting case of helicity-conserving media is governed by principles otherwise protecting extended surface states of topological insulators or Weyl semimetals. This correspondence manifests itself in the Chern-Simons theory outlined above and implies the absence of Anderson localization in sectors of definite helicity. We note that in the optical context, this protection mechanism engages longitudinal electromagnetic modes, which are absent in both vacuum and electronic systems. This finding underscores the importance of longitudinal modes for light delocalization, highlighted from a different perspective in ref. 30 and demonstrated in the recent numerical simulations[8].

Intermediate disorder: anomalous transport

Weyl semimetals show various anomalies in electronic transport, among them the *chiral magnetic effect*—an electric current driven by the application of a static magnetic field. The analog of a magnetic field required for its optical variant, the *helical vortical effect*[31–33], has been proposed for meta-materials, such as resonator lattices[34,35] and magnetoelectric materials[31]. We here consider their realization in systems in rotational motion[36], such as cylinders of radius R and length L, rotated around their axis at uniform angular velocity Ω. In the rotating frame, Maxwell's equations for waves of frequency ω become equivalent to the Schrödinger equation for a spin-1 Weyl fermion subject to a magnetic field $B = \frac{1-\epsilon\mu}{c^2}\omega\Omega$ along the cylinder axis. In the presence of disorder, the Chern-Simons theory applied to this geometry predicts a succession of three qualitatively different regimes, marked by length scales $l_B < l_h$: For cylinder lengths $L < l_B \equiv \sigma/(8B)$, the transmission is Ohmic with a length dependence $T \simeq \pi R^2\sigma/L$. Here, σ and T are the optical analogs of the medium's conductivity and conductance, respectively. At the scale l_B a crossover into a regime with length-independent transmission $T = N_\phi/2\pi$ occurs, where $N_\phi = \pi R^2 B$ is proportional to the magnetic field and plays a role analogous to the number of "flux quanta" threading the system. Physically, this crossover reflects a change from diffusive light propagation at short scales to the *drift* of two transport channels of opposite helicity at larger scales. Remarkably, this mechanism leads to immunity against Anderson localization, including in elongated quasi-one-dimensional geometries where localization is generally strong and occurs even for weak disorder. Drift transport prevails until helicity mixing at the scale l_h leads into another regime of Ohmic $T \sim 1/L$, and eventually localized $T \sim \exp(-L/\xi)$ transport. These regimes may be observable in scattering experiments monitoring light transmission either as a function of length or, perhaps more conveniently, sample rotation frequency, see also Fig. 2.

Weak disorder: effectively clean phases

The construction of the field theory outlined above relies on a finite self-consistently obtained scattering rate κ. Pioneering work[37,38] has shown that in the long wavelength limit, $\lambda \to \infty$, there exists a quantum critical point marked by a disorder strength $w = 2\pi^2/\Lambda$ below which the self-consistent scattering rate *vanishes*. Here, Λ^{-1} is a small distance cutoff to be identified with the correlation range of the disorder (see below). For lower concentrations, renormalized perturbation theory[37] around the Weyl nodal point reveals that scattering becomes irrelevant: long-wavelength propagation modes effectively average over medium fluctuations and pass them unhindered. For finite wavelengths, a fan-like critical region emerges above the critical point. Helicity-conserving optical (meta)materials may provide the required homogeneity levels to realize the weak scattering universality class, where a system looks "effectively transparent" in the long wavelength limit. They may also define an ideal platform to study its behavior under changes in disorder concentration or light frequency. We finally note that the existence of a quantum critical

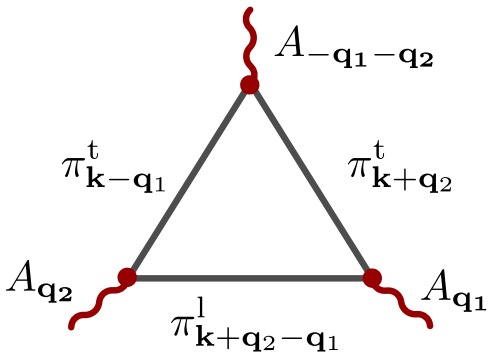

Fig. 3 | Triangle scattering amplitude. A Feynman diagram contributing to the A^3-term in the Chern-Simons action Eq. (7). Three slow fields A of low characteristic wave-vectors $\mathbf{q}_i \ll \Lambda$ are connected by electromagnetic field propagators, one of which needs to be a longitudinal mode. The integral over wave-vectors $\mathbf{k}$ is dominated by large $|\mathbf{k}| \sim \Lambda$, where the influence of disorder on the latter is exceptionally strong.

point between two phases at low disorder and large wavelength is a specific feature of the Weyl universality class, different from the generic feature that scattering becomes less effective in long wavelength limits[39,40].

Microscopic analysis

In the following, we outline the derivation of the results above, starting from the source-free Maxwell equations for electromagnetic waves with frequency ω (summation convention)

$$\partial_i D_i = 0, \qquad \epsilon_{ijk}\partial_j E_k = \frac{i\omega}{c} B_i, \tag{2}$$

$$\partial_i B_i = 0, \qquad \epsilon_{ijk}\partial_j H_k = -\frac{i\omega}{c} D_i. \tag{3}$$

The presence of a scattering medium enters through the relations $B_i = \mu H_i$, $D_i = \epsilon E_i$ where the magnetic permeability $\mu_{\mathbf{x}}$ and permittivity $\epsilon_{\mathbf{x}}$ are randomly fluctuating, and c is the velocity of light in vacuum.

The standard approach to wave localization[28,41] combines Eqs. (2) and (3) to a single random wave equation for the electric field, resembling a Schrödinger equation in a random potential. However, following ref. 42, we work here in an alternative representation, emphasizing two crucial aspects of light: linear dispersiveness and helicity. To this end, we introduce the rescaled field vectors $\mathcal{E}_i = \sqrt{\epsilon}E_i$ and $\mathcal{H}_i = \sqrt{\mu}H_i$, along with the left and right circular polarized amplitudes $\Phi^{\pm} = (\mathcal{E} \pm i\mathcal{H})/\sqrt{2n}$, where $n = \sqrt{\epsilon\mu}$ the (local) refractive index. It is then straightforward to show (see methods and ref. 42) that the six-component field vector $\Phi = (\Phi^+, \Phi^-)$ obeys the Dirac-like equation

$$\left(-i\tau_3 \otimes c\partial\!\!\!/ - \tau_1 \otimes c\phi\!\!\!/_Z + V\right)\Phi = \omega\Phi. \tag{4}$$

Here, the matrices τ_i act between the helical subspaces of the Φ-vector and we use a variant of the Feynman slash notation, $\phi\!\!\!/ = v_i S_i$, where $(S_j)_{\alpha\beta} = -i\epsilon_{j\alpha\beta}$ are three-dimensional anti-symmetric matrices acting on the helical components $\Phi^{\pm}$ of the field vector separately. Their commutation relations $[S_i, S_j] = i\epsilon_{ijk}S_k$ and the normalization $S_iS_i = 2\mathbb{1}_3$ identify them as spin-1 operators heralding the nature of the photon that would emerge upon quantization of the theory[42,43]. Randomness enters the problem through the scalar potential $V_{\mathbf{x}} = \omega(1 - n_{\mathbf{x}})$ and vector potential

$$\phi\!\!\!/_{Z,\mathbf{x}} = \tfrac{1}{2}\partial\!\!\!/ \ln Z_{\mathbf{x}}.$$

In the absence of impedance fluctuations, $Z_{\mathbf{x}} = \text{const.}$, or $\phi\!\!\!/ = 0$, the equation splits into two blocks,

$$\left(\mp ic\partial\!\!\!/ + V\right)\Phi^{\pm} = \omega\Phi^{\pm}, \tag{5}$$

describing the independent propagation of fields of opposite helicity. Upon rescaling by $\hbar$, it becomes identical to the Weyl equation of spin-1 states[20,44,45]. In condensed matter physics, spin-1 Weyl states have been identified as low-energy quasi-particles featuring at the band crossing points of crystals with nontrivial space group symmetries[20]. In the clean case, $V = 0$, Eq. 5 describes two linearly dispersive bands, plus a flat band of zero-energy quantum states. The two nontrivial bands carry an integer topological index $C = \pm 2$ obtained, e.g., by integration of the Berry curvature of eigenstates $\Phi^{\pm}$ in momentum space over closed surfaces surrounding $p = 0$. The presence of these quantum numbers is at the heart of topological protection against localization in the presence of disorder. In optics, the topologically charged bands represent transverse modes of the electromagnetic field, labeled by their propagation wave-vector, and the degenerate band corresponds to longitudinal modes. While the latter are irrelevant in vacuum, they open a transmission channel in random media that becomes effective at subwavelength scales, thereby hindering localization[8,30]. As we will discuss next, this mechanism draws upon the interplay between transverse and longitudinal fluctuations, highlighting their interplay in random light scattering.

Chern-Simons theory

In quantum physics, the multiple wave interference processes culminating in Anderson localization at large length scales are described by field theories whose degrees of freedom, $T(\mathbf{x})$, are matrices reflecting the symmetries of a given problem[46,47]. The transfer of these methods to light scattering was pioneered in refs. 27–29, with the prediction that length scales exceeding the mean free scattering path, κ^{-1}, are described by the action

$$S_0[Q] = \frac{\sigma}{16}\int d^3x\, \mathrm{tr}(\partial Q \partial Q), \tag{6}$$

where $Q = T\sigma_3 T^{-1}$, here and throughout unlabeled Pauli matrices σ_i act in a two-dimensional multiplet space distinguishing between advanced and retarded wave propagation, and the constraint $Q^2 = \mathbb{1}$ identifies the action as that of a nonlinear σ-model. The coupling constant $\sigma = (\omega^2 + 3\kappa^2)\left(\omega^2 - \frac{1}{3}\kappa^2\right)/\left(\pi\kappa(\omega^2 + \kappa^2)\right)$ depends on frequency and κ^{-1} (see the "Methods" section), and it determines the optical transmission properties at large length scales: depending on whether $\sigma\kappa^{-1}$ is large or small compared to unity, Eq. (6) describes the flow into a diffusive or a localized phase, the two scenarios being separated by the Anderson localization transition[48].

Our resolution of distinct helical sectors changes this result. Instead of a single slow field, we now have two, $Q_{\pm}$, describing propagation in channels of opposite helicity via actions $S_{\pm}[Q_{\pm}] = S_0[Q_{\pm}] \pm S_{\mathrm{top}}[A_{\pm}]$. Alongside the standard gradient action $S_0[Q_{\pm}]$, these contain a topological action of Chern-Simons form $S_{\mathrm{top}}[A_\chi] = S_{\mathrm{CS}}[A^+_\chi] - S_{\mathrm{CS}}[A^-_\chi]$, where

$$S_{\mathrm{CS}}[A] = -\frac{i\epsilon_{ijk}}{8\pi}\int d^3x\, \mathrm{tr}\left(A_i\partial_j A_k + \frac{2}{3}A_iA_jA_k\right), \tag{7}$$

$A^s_\chi = T^{-1}_\chi \partial T_\chi P^s$, and $P^s = \frac{1}{2}(\mathbb{1} + s\sigma_3)$ are projectors on retarded or advanced propagation channels.

To rationalize the emergence of this term, consider the unitaries $T_{\pm}$ as nonabelian gauge transformations. Our theory then resembles that of three-dimensional Dirac fermions coupled to vector potentials $\mathbf{A} = T^{-1}\partial T$. This system is subject to the parity anomaly[49], where ultraviolet singularities require giving up parity symmetry in exchange for maintained gauge

Table 1 | Material parameters

Refractive index	$\langle \boldsymbol{V}_{\mathbf{x}} \boldsymbol{V}_{\mathbf{x}'} \rangle = \boldsymbol{wc^2}\delta(\mathbf{x}-\mathbf{x}')$
Impedance	$\langle \boldsymbol{a}_{i,\mathbf{x}} \boldsymbol{a}_{j,\mathbf{y}} \rangle = \boldsymbol{\gamma\delta(x-y)\delta_{ij}}$
Scattering rate	$\kappa = \kappa(w, \Lambda, \omega)$
Transmission coefficient	$\sigma = \sigma(\omega, \kappa)$
Helicity coupling	$\Gamma_{\rm h} = 6\gamma(\kappa/wc)^2$
Helical length	$l_{\rm h} \sim (\sigma/\gamma)^{1/2} wc/\kappa$

Parameters derived from variances of the potential, V and vector potential, a_i, generated by the refractive index, respectively, include the gradient of the impedance. See also Eqs. (1) and around Eq. 4 for definitions and further discussion.

invariance. On general grounds, this principle requires the presence of a Chern-Simons term in gauge field actions.

Referring to the "Methods" section for details, the CS term reflects the presence of "triangle" scattering amplitudes[49], coupling three photon propagators to the gauge field, see Fig. 3. We find that these amplitudes necessarily involve the coupling of transverse photon propagators to spin $S_z = 0$ longitudinal propagators. What is more, the dominant contributions come from high-lying wave-vectors of the order of the UV-cutoff Λ, which is the parameter region dominantly supporting longitudinal propagators. These observations underscore the importance of longitudinal modes in the physics of light delocalization, pointed out from a different perspective in refs. 8,30.

The derivation of this effective theory answers the questions raised above. The low-energy theory, split into two helical sectors $S[Q_+, Q_-] = S_+[Q_+] + S_-[Q_-]$, is mathematically identical to that of Weyl quantum matter in the absence of inter-node scattering[24,26]. An independent way of rationalizing its protection against localization makes reference to the bulk-boundary principle of topological quantum matter: individual of the Chern-Simons actions $S_\pm$ describe isolated surfaces of four-dimensional topological insulators[50], where localization is excluded via a spectral flow principle[25]. Our derivation of the CS action generalizes this result, previously established for spin-1/2 states, to spin-1. Interestingly, the protection mechanism extends to quasi-one-dimensional 'waveguide' geometries[24], where localization would otherwise be unavoidable regardless of the value of σ.

To find out what happens once impedance Z-fluctuations couple the helicity sectors, we need to be more explicit concerning the realization of randomness. Assuming scattering centers smaller than the wavelength, $\Lambda^{-1} < c/\omega$, we consider Gaussian variances as in the first two rows of Table 1, with δ-functions defined to be smeared over scales Λ^{-1}. The light scattering rate $\kappa(w, \Lambda, \omega)$, and the light transmission $\sigma = \sigma(\omega, \kappa)$ depend on these parameters in a manner that can be computed via self-consistent Born approximation, but will not be essential for us. Presently, the most important parameter is a *helicity coupling constant* $\Gamma_{\rm h}$ whose dependence on impedance fluctuations and the density of scattering modes is stated in Table 1. This constant enters the theory via the term

$$S_{\rm c}[Q] = \Gamma_{\rm h} \int d^3x \, {\rm tr}(Q_+ Q_-), \tag{8}$$

coupling the two helical fields. At large length scales, Eq. (8) enforces a locking $Q_+ = Q_- \equiv Q$. Inspection of the sign structure of the CS terms shows that they cancel out in this limit.

To parametrically estimate the corresponding crossover scale $l_{\rm h}$, we compare the characteristic value of the diffusion action $\sim\sigma l^3/l^2$ to that of the helicity action $\sim\Gamma_{\rm h} l^3$ at length scales l. Equating these values, we obtain $l \equiv l_{\rm h} \sim \sqrt{\sigma/\Gamma_{\rm h}}$. Above this length scale, the theory will flow into an Anderson localized phase, provided the bare transmission coefficient $\sigma(\omega, \kappa)$ is supercritically weak.

Generalized for the presence of a synthetic magnetic field B, the theory is defined by Eqs. (6),(7), and (8) predict a number of intriguing transport phenomena. Referring to ref. 24 for details, the vector potentials entering the CS term $A_i \to A_i + A_{{\rm e},i}$ must then be interpreted as the sum of the fluctuation fields and the potential $A_{{\rm e},i}$ representing B. In this case, it becomes a one-derivative operator describing *drift* along quasi one-dimensional geometries aligned with the field[24]. A dimensional estimate shows that for lengths exceeding the crossover scale l_B the drift action dominates over the diffusive Eq. (6) causing a crossover from 'Ohmic' to constant transmission (see Fig. 2). Only at scales $L > l_{\rm h}$, the helical drift terms cancel out, and we re-enter an Ohmic, and eventually an Anderson localized regime. We here assumed a hierarchy of scales $l_B < l_{\rm h}$ corresponding to weak helicity breaking. In the opposite case, the CVE will be unobservable in a disordered medium.

Experimental realizability

Before concluding, let us speculate on the experimental accessibility of the phenomena discussed above. Again, the situation calls for a separate consideration of strong, intermediate and weak disorder. Beginning with the latter, weakly disordered meta-materials with approximately dual scatterers have been theoretically[51] and experimentally studied[52]. Specifically, the 'first Kerker condition'[23] is realized in dielectric sub-wavelength spheres whose scattering profile was found[21,22] to be indistinguishable from that of dual magneto-dielectric spheres. Silicon (and other semiconductor materials such as germanium and rutile-TiO_2[22]) are likewise close to a near-dual limit for certain frequency ranges of the scattering light. Refs. 53–55 noted the persistence of circular polarization indicative of a dual limit in resonant dielectric Mie particles with high magnetic polarizability.

The limit of strong helicity-conserving scattering, on the other hand, may be elusive in these present-day materials. For one, the Kerker condition holds only for narrow frequency ranges, defined by specific ratios between scatterer size and light wavelength, thus constraining the size distribution of scatterers in random media, cf.[51]. Second, higher-order multipolar responses compromising helicity may become effective via proximity effects in closely packed materials. In view of this situation, the weak and intermediate regimes appear to be most accessible at present.

We suggested probing this regime in cylindrical geometries rotating with angular velocity Ω. Assuming sample radii R in the centimeter range, and transmission coefficients $T = \pi R^2 \frac{\sigma}{L}$ of the order of unity, the crossover length $l_B \sim \frac{\sigma c^2}{8\omega\Omega}$ will be comparable to the system size for rotation frequencies down by a factor $(\lambda/R)^2$ relative to the frequency of light, ω. For example, for a wavelength in the visible range, $\lambda \sim 500$ nm, and including numerical factors, we obtain characteristic frequencies Ω in the kHz range, which may be technically achievable. We also note that in the rotating frame, an incoming cylindrically symmetric wave front will be perceived as stationary, showing that effects related to the scattering off non-stationary scatterers can be avoided in this setting. However, in view of the remaining experimental challenges, large-scale numerical simulations as in refs. 31–35 will be natural first steps in targeting topological phenomena in the weak and intermediate disorder regime.

Conclusions

The scattering of light in random media is commonly discussed within the framework of the Anderson universality class, with additional account for the vectorial nature of electromagnetic waves. Here, we have shown that the linear dispersion of electromagnetic waves, combined with its vector nature, implies more far-reaching departures from standard localization theory. It puts the problem into the universality class of the random spin-1 Weyl semimetal, where the role of Weyl cones of opposite chirality is taken by waves of opposite helicity. As a consequence, the transmission of light will show sensitivity to the degree of helicity mixing. We introduced Chern-Simons theory as a universal framework for the description of the ensuing phenomena at length scales exceeding the scattering mean free path. We used this platform to discuss three manifestations of the equivalence to the quantum Weyl problem: Topological protection against localization in the limiting case of strong helicity preserving disorder, transmission anomalies caused by an interplay of intermediate strength disorder and the chiral

vortical effect, and the emergence of "effectively clean" phases in which the presence of a weak concentration of scattering centers becomes irrelevant in a quantum phase transition. In view of the comparatively high level of control available in optical meta-materials, the observability of such phenomena may be less challenging than in the exotic crystalline quantum materials harboring condensed matter realizations of spin-1 Weyl cones. Perhaps, light scattering may even become an efficient macroscopic analog simulator of universal phenomena predicted, but so far unobserved in Weyl quantum transport.

Methods

Throughout this section, we set $c = 1$ for notational simplicity.

'Dirac' equation for photons

We start by defining the six-component vector $\Psi = E \oplus H$, and the diagonal matrix $D = \epsilon \mathbb{1} \oplus \mu \mathbb{1}$, to write Maxwell's equations as

$$i\partial_t D\Psi = \tau_2 i\partial\!\!\!/ \Psi,$$

where τ_2 acts in the electric/magnetic subspace of Ψ, and the action of the differential operator on three-component vectors is defined through the slash notation $(\partial\!\!\!/ X)_k = i\epsilon_{klm}\partial_l X_m$, or $\partial\!\!\!/ X = S_l \partial_l X$, with the hermitian matrices $(S_l)_{mk} \equiv i\epsilon_{mlk}$. Assuming harmonic time dependence of Ψ with characteristic frequency ω, the equation reduces to $\omega\Psi = D^{-1}\tau_2(-i\partial\!\!\!/)\Psi$. We next apply a similarity transformation, $\Psi = D^{-1/2}\tilde{\Phi}$, to obtain the representation

$$\omega\tilde{\Phi} = D^{-1/2}\tau_2(-i\partial\!\!\!/)D^{-1/2}\tilde{\Phi}.$$

The operator on the r.h.s. is manifestly hermitian (safeguarding the existence of solutions with real frequencies ω) but inconvenient to work with as the scattering disorder is hiding in the factor matrices D. We aim to bring it into a more customary form 'derivative operator + disorder potential'. To this end, we first represent the matrix D in terms of the refractive index and impedance as $D = n\exp(\ln Z\tau_3)$, leading to

$$\omega n\Phi = \left(-i\partial\!\!\!/\tau_2 - \frac{\tau_1}{2}(\partial\!\!\!/ \ln Z)\right)\Phi,$$

where $\Phi = n^{-1/2}\tilde{\Phi}$. Finally, with $V = \omega(1 - n)$, and

$$\phi\!\!\!/_Z \equiv \tfrac{1}{2}\partial\!\!\!/ \ln Z$$

we obtain the desired form of the equation,

$$\omega\Phi = \left(-i\partial\!\!\!/\tau_2 - \tau_1\phi\!\!\!/_{Z,\mathbf{x}} + V_{\mathbf{x}}\right)\Phi.$$

Performing a unitary rotation around τ_1 to the helical eigenstates $\Phi \to (\Phi^+, \Phi^-)$, we arrive at Dirac-like equation stated in the text.

Replica field theory

We here provide details concerning the derivation of the Chern-Simons field theory discussed in the main text. Referring to rref. 24 for a more detailed exposition, our discussion will be succinct but self-contained. Specifically, we highlight departures from the theory of the spin 1/2-system. Alongside the presence of longitudinal modes, these include a different behavior under physical time reversal: while for spin-1/2 time reversal squares to minus the identity, it is even in the spin-1 case. This puts our problem into the symmetry class AI (otherwise known as the Wigner-Dyson orthogonal class) in the nomenclature of refs. 56,57. A detailed account of the calculations, including all intermediate steps, can be found in the Supplementary Notes 1 and 2.

The starting point of the field theory description is the replica partition function,

$$\mathcal{Z}[j] = \int D\psi \left\langle e^{i\int d^3x\, \bar{\psi}(i\delta\sigma_3 + \omega - \tau_3 \otimes \mathbf{k}\!\!\!/ - V)\psi} \right\rangle_{\rm dis}, \tag{9}$$

where $\psi = \{\psi_{s,\sigma,a,\nu,\chi}(\mathbf{x})\}$ is a $(2 \times 2 \times R \times 3 \times 2)$ component Grassmann field. Here, $s = 1, 2$ is a two-component index distinguishing between retarded and advanced fields, $a = 1, \ldots, R$ is a replica index, $\nu = 1, 2, 3$ labels the spin degree of freedom, and $\chi = \pm$ helicity. The last remaining index, $\sigma = 1, 2$, accounts for time-reversal symmetry, which is realized via the relation $\bar{\psi} = (i\sigma_2^{\rm tr}\psi)^T$. Finally, $\sigma_i^{\rm tr}$ and σ_i are Pauli matrices in the spaces of σ- and s-indices, respectively.

The action in Eq. 9 possesses a continuous symmetry which will be crucial for all what follows: it is invariant under uniform rotations $\psi \to T\psi$, $\bar{\psi} \to \bar{\psi}T^{-1}$ commuting with $\tau_3 \otimes \mathbf{k}\!\!\!/$. These are spatially uniform rotations structureless in spin-indices $\nu = 1, 2, 3$, and diagonal in helical τ-space. Consistency with the time reversal structure relating ψ and $\bar{\psi}$ implies the further constraint $T^T = \sigma_2^{\rm tr}T^{-1}\sigma_2^{\rm tr}$, identifying T as an element of the symplectic group Sp(4R).

Hubbard-Stratonovich decoupling: the Gaussian average over fluctuations V in Eq. 9 generates a quartic 'interaction term', local in space but with tensor structure in the 'internal' indices s, σ, a, ν, χ. We decouple this term by a matrix-field $Q = \{Q^{ss',\sigma\sigma',aa'}_{\chi\chi',\nu\nu'}\}$ via Hubbard-Stratonovich transformation and subsequently perform the quadratic integral over ψ to obtain the matrix field partition sum $\mathcal{Z} = \int dQ e^{-S[Q]}$, with

$$S[Q] = \frac{1}{2w}\mathrm{Tr}\, Q^2 - \frac{1}{2}\mathrm{Tr}\ln\left(\omega - \tau_3 \otimes \mathbf{k}\!\!\!/ + i\delta\sigma_3 + iQ\right).$$

Mean-field analysis: variation of the action in Q leads to the saddle point equation,

$$Q = \frac{iw}{2}\int^{\Lambda}(dk)\,\frac{1}{\omega - \tau_3 \otimes \mathbf{k}\!\!\!/ + i\delta\sigma_3 + iQ}, \tag{10}$$

where $(dk) \equiv d^3k/(2\pi)^3$ and the superscript Λ indicates that the formally divergent momentum integration is to be cut off at the inverse of the correlation length Λ^{-1} implicit in the definition of our disorder correlators. We assume this to be the smallest length scale in the problem, in particular, $\Lambda^{-1} \ll c/\omega$.

The structure of the equation indicates that the mean field Q plays the role of a self-consistent Born "self-energy" of light propagators picked up upon scattering. The detailed solution of this equation will lead to a self-energy operator with structure in spin space (ν), reflecting differences between longitudinal and transverse self-energies. While these are important for the quantitative solution computation of scattering cross-sections, they have no qualitative significance for our analysis. We therefore seek an approximate solution in terms of the spin-isotropic ansatz $Q = \kappa\sigma_3$ (an imaginary part of Q can be absorbed by a shift in frequency and will be inessential for us, while the real part κ defines the scattering mean free path), where the Pauli matrix reflects the causal increment $i\delta\sigma_3$. Substituting it into the equation above and tracing over spin indices we obtain

$$\kappa = -\frac{w}{2}\mathrm{Im}\int(dk)\left(\frac{2}{3}\frac{\omega + i\kappa}{(\omega + i\kappa)^2 - k^2} + \frac{1}{3}\frac{1}{\omega + i\kappa}\right). \tag{11}$$

The detailed solution of the equation then leads to a function $\kappa = \kappa(w, \omega, \Lambda)$. However, for our purposes, it will be sufficient to neglect these parametric dependencies, as we are working at fixed values of the argument parameters.

Soft mode action: we next recall that the action of the matrix integral, possessed a continuous symmetry under Sp(4R) transformations T_χ block diagonal in helical space. Following the standard Goldstone mode paradigm, we promote these transformations to modes $T_{\chi\mathbf{x}}$ fluctuating in real space, and consider the generalized mean field configurations

$\kappa T_\chi \sigma_3^{ra} T_\chi^{-1} \equiv Q_\chi$. Here, the Goldstone modes Q_χ, which are the effective degrees of freedom of the nonlinear σ-model of localization theory for symmetry class AI, take values in the coset space $\mathrm{Sp}(4R)/\mathrm{Sp}(2R) \times \mathrm{Sp}(2R)$[58]. (The division of the factor group accounts for the fact that transformations commuting with σ_3 are unbroken symmetries, much like rotations around the magnetization-axis in a ferromagnetic material.) The symmetry under time reversal discussed above is inherited by the Q's in the form $Q_\chi^T = \sigma_2^{\mathrm{tr}} Q_\chi \sigma_2^{\mathrm{tr}}$.

With these degrees of freedom, the effective action becomes a sum of two helical contributions $\mathcal{Z} = \int D(T_+, T_-) e^{-S[T_+]-S[T_-]}$, with

$$S[T_\chi] = -\frac{1}{2}\mathrm{Tr}\ln\left(\omega - \chi \not{k} + i\kappa T_\chi \sigma_3 T_\chi^{-1}\right). \tag{12}$$

Where 'Tr' is a trace over internal degrees of freedom and space. A naively applied similarity transformation under the 'trace-log', $\mathrm{Trln}(\ldots) \to \mathrm{Trln}\left(T_\chi^{-1}(\ldots)T_\chi\right)$, would lead to a putatively equivalent expression in terms of $\not{A}_\chi \equiv S_i A_{\chi,i} \equiv S_i T_\chi^{-1}\partial_i T_\chi$. However, this operation is premature because the similarity transformation of the UV singular Dirac like operator under the trace is subject to the parity anomaly[49]. One way to handle the situation[24,59] is to consider

$$S[T_\chi] = -\frac{1}{2}\mathrm{Tr}\ln\left(\omega + i\kappa\sigma_3 - \chi\not{k} - i\chi\not{A}_\chi\right) - S_\eta[T_\chi], \tag{13}$$

where $S_\eta[T_\chi] = \frac{1}{2}\mathrm{Tr}\ln\left(i\eta\sigma_3 - \chi\not{k} - i\chi\not{A}_\chi\right)$ with $\eta \to 0$ is introduced to regularize UV divergences at large $\not{k}$.

Gradient expansion: the final construction step is the expansion up to third order in the spatial gradients contained in $\not{A}_\chi$. Inspection of the logarithm shows that the expansion actually is in the combination $G_\chi \not{A}_\chi$, where $G_\chi \equiv (\omega + i\kappa\sigma_3 - \chi\not{k})^{-1}$ is the photon propagator coupled to the SCBA scattering self-energy. To proceed, it is convenient to decompose G_χ into longitudinal and transverse modes. Introducing the projection operators $\pi_{\mathbf{k}}^{\mathrm{l}} = \mathbf{k}\mathbf{k}^T/k^2$ and $\pi_{\mathbf{k}}^{\mathrm{t}} = 1 - \pi_{\mathbf{k}}^{\mathrm{l}}$, it is straightforward to verify that $G_{\chi k} = G_{\mathrm{t},\chi,\mathbf{k}}\,\pi_{\mathbf{k}}^{\mathrm{t}} + G_{\mathrm{l}}\,\pi_{\mathbf{k}}^{\mathrm{l}}$, with

$$G_{\mathrm{t},\chi,\mathbf{k}} = \frac{\omega + i\kappa\sigma_3 + \chi\not{k}}{(\omega + i\kappa\sigma_3)^2 - k^2}, \qquad G_{\mathrm{l}} = \frac{1}{\omega + i\kappa\sigma_3}. \tag{14}$$

With this decomposition, it is a matter of a straightforward, if tedious computation to first take the traces over the three-dimensional spin representation space, and then integrate over momenta. As a result, we obtain a symmetric second order $(\partial_i\partial_i)$ and a fully antisymmetric third order $(\epsilon_{ijk}\partial_i\partial_j\partial_k)$ combination of derivatives acting on the slow fields of the theory, T. The first of these is weighted by products $G_{\mathrm{t}}G_{\mathrm{t}}$ and $G_{\mathrm{t}}G_{\mathrm{l}}$, whose momentum integral yields the coefficient σ stated in the main text. At third order, we obtain a coefficient $G_{\mathrm{t}}G_{\mathrm{t}}G_{\mathrm{l}}$, the product of three propagators defining the 'triangle graph' of a Chern-Simons term (cf. Fig. 3 and ref. 49). One of these is a longitudinal mode, highlighting the importance of the non-dispersive 'flat band' in the localization physics of the spin-1 Weyl system. The momentum integral over these propagators yields the universal coefficient multiplying Eq. (7), required on general grounds for a Chern-Simons action. For a full exposure of the lengthy calculations leading to these results, we refer to the Supplementary Note 2.

Helicity mixing: we finally include the helicity-mixing $\tau_1\phi_Z$ operator into the analysis. With $\not{A}_Z \equiv T^{-1}\tau_1\phi_Z T$ and block diagonal $T = T_+ \oplus T_-$, we consider the unitarily transformed from a locally varying impedance,

$$S[T] = -\frac{1}{2}\mathrm{Tr}\ln\left(\omega + i\kappa\sigma_3 - \tau_3\not{k} + \not{A}_Z + \ldots\right),$$

where the ellipses denote T-dependent contributions previously accounted for in the gradient expansion. We expand to second order in $\not{A}_Z$, and average over the distribution given in Table 1, to arrive at the effective quadratic coupling action

$$\begin{aligned} S_{\mathrm{h}}[T] &= -\frac{\gamma}{4}\int d^3x\,\mathrm{tr}\left(TG_{\mathbf{x},\mathbf{x}}T^{-1}\tau_1 S_i T G_{\mathbf{x},\mathbf{x}} T^{-1}\tau_1 S_i\right) \\ &= \left(\frac{2\kappa}{w}\right)^2 \times \frac{3\gamma}{4}\int d^3x\,\mathrm{tr}\left(Q\tau_1 Q\tau_1\right), \end{aligned}$$

where $G = G_+ \oplus G_-$. In passing from the first to the second line, we used that the Green functions $G_\chi(\mathbf{x},\mathbf{x}) = \int (dk) G_{\chi,k}$ solve the mean field equation, i.e., $G(\mathbf{x},\mathbf{x}) = (-2\pi i\kappa/w)\sigma_3$. Tracing over helical space we then arrive at Eq. (8) in the main text, with the coupling constant Γ_{h} specified in Table 1.

Limits of applicability: we conclude with some comments on the validity of the effective field theory. The discussion of the applicability of the nonlinear sigma model in the strong scattering regime has a long history and remains a topic of debate (for a recent critical contribution, see e.g., ref. 60). However, there appears to be a consensus that in the absence of topological effects the Anderson transition follows a one-parameter scaling hypothesis adequately described by a renormalization group approach to the sigma model in $2 + \epsilon$ dimensions.

Topological terms in these theories stand on a more solid footing as their presence follows entirely on the basis of symmetries[57], independent of specific details such as disorder strength. However, by the same principle, effects characterizing "symmetry-protected topological phases" generally depend on the presence of certain symmetries. For example, magnetic fields compromise topological protection in time-reversal invariant topological insulators, technically by gapping out topological terms. An analogous scenario is realized here where topological protection is guaranteed, unless helicity symmetry is broken in a manner similar to spin rotation invariance breaking in quantum theories.

Data availability

Data sharing is not applicable to this article as no datasets were generated or analyzed during the current study.

Received: 15 October 2024; Accepted: 15 June 2025;
Published online: 15 July 2025

References

1. Gomard, G., Peretti, R., Drouard, E., Meng, X. & Seassal, C. Photonic crystals and optical mode engineering for thin film photovoltaics. *Opt. Express* **21**, A515–A527 (2013).
2. Cernuto, G., Masciocchi, N., Cervellino, A., Colonna, G. M. & Guagliardi, A. Size and shape dependence of the photocatalytic activity of TiO_2 nanocrystals: a total scattering Debye function study. *J. Am. Chem. Soc.* **133**, 3114–3119 (2011).
3. Cao, H. Review on latest developments in random lasers with coherent feedback. *J. Phys. A Math. Gen.* **38**, 10497 (2005).
4. Wiersma, D. S. The physics and applications of random lasers. *Nat. Phys.* **4**, 359–367 (2008).
5. Andreasen, J. et al. Modes of random lasers. *Adv. Opt. Photon.* **3**, 88–127 (2011).
6. Oliver, J. T., Crane, T. & Sapienza, L. Optical sensing with Anderson localized light. *Appl. Phys. Lett.* **111**, 141103 (2017).
7. Skipetrov, S. E. & Page, J. H. Red light for Anderson localization. *N. J. Phys.* **18**, 021001 (2016).
8. Yamilov, A. et al. Anderson localization of electromagnetic waves in three dimensions. *Nat. Phys.* https://doi.org/10.1038/s41567-023-02091-7 (2023).

9. Condat, C. A. & Kirkpatrick, T. R. Observability of acoustical and optical localization. *Phys. Rev. Lett.* **58**, 226–229 (1987).
10. Hu, H., Strybulevych, A., Page, J. H., Skipetrov, S. E. & van Tiggelen, B. A. Localization of ultrasound in a three-dimensional elastic network. *Nat. Phys.* **4**, 945–948 (2008).
11. Flores, J. et al. Anderson localization in finite disordered vibrating rods. *Europhys. Lett.* **101**, 67002 (2013).
12. Ángel, J. C., Guzmán, J. C. T. & de Anda, A. D. Anderson localization of flexural waves in disordered elastic beams. *Sci. Rep.* **9**, 3572 (2019).
13. Chabé, J. et al. Experimental observation of the Anderson metal-insulator transition with atomic matter waves. *Phys. Rev. Lett.* **101**, 255702 (2008).
14. Lemarié, G., Lignier, H., Delande, D., Szriftgiser, P. & Garreau, J. C. Critical state of the Anderson transition: between a metal and an insulator. *Phys. Rev. Lett.* **105**, 090601 (2010).
15. Billy, J. et al. Direct observation of Anderson localization of matter waves in a controlled disorder. *Nature* **453**, 891–894 (2008).
16. Roati, G. et al. Anderson localization of a non-interacting Bose-Einstein condensate. *Nature* **453**, 895–898 (2008).
17. White, D. H. et al. Observation of two-dimensional Anderson localisation of ultracold atoms. *Nat. Commun.* **11**, 4942 (2020).
18. Schwartz, T., Bartal, G., Fishman, S. & Segev, M. Transport and Anderson localization in disordered two-dimensional photonic lattices. *Nature* **446**, 52–55 (2007).
19. De Raedt, H., Lagendijk, A. & de Vries, P. Transverse localization of light. *Phys. Rev. Lett.* **62**, 47–50 (1989).
20. Bradlyn, B. et al. Beyond Dirac and Weyl fermions: unconventional quasiparticles in conventional crystals. *Science* **353**, aaf5037 (2016).
21. García-Etxarri, A. et al. Strong magnetic response of submicron silicon particles in the infrared. *Opt. Express* **19**, 4815–4826 (2011).
22. Geffrin, J. M. et al. Magnetic and electric coherence in forward- and back-scattered electromagnetic waves by a single dielectric subwavelength sphere. *Nat. Commun.* **3**, 1171 (2012).
23. Kerker, M., Wang, D.-S. & Giles, C. L. Electromagnetic scattering by magnetic spheres. *J. Opt. Soc. Am.* **73**, 765–767 (1983).
24. Altland, A. & Bagrets, D. Theory of the strongly disordered Weyl semimetal. *Phys. Rev. B* **93**, 075113 (2016).
25. Altland, A. et al. Fragility of surface states in non-Wigner-Dyson topological insulators. *Phys. Rev. X* **14**, 011057 (2024).
26. Altland, A. & Bagrets, D. Effective field theory of the disordered Weyl semimetal. *Phys. Rev. Lett.* **114**, 257201 (2015).
27. John, S. Strong localization of photons in certain disordered dielectric superlattices. *Phys. Rev. Lett.* **58**, 2486–2489 (1987).
28. John, S. Electromagnetic absorption in a disordered medium near a photon mobility edge. *Phys. Rev. Lett.* **53**, 2169–2172 (1984).
29. John, S. Localization and absorption of waves in a weakly dissipative disordered medium. *Phys. Rev. B* **31**, 304–309 (1985).
30. van Tiggelen, B. A. & Skipetrov, S. E. Longitudinal modes in diffusion and localization of light. *Phys. Rev. B* **103**, 174204 (2021).
31. Hayata, T. Chiral magnetic effect of light. *Phys. Rev. B* **97**, 205102 (2018).
32. Fukushima, K., Kharzeev, D. E. & Warringa, H. J. Chiral magnetic effect. *Phys. Rev. D.* **78**, 074033 (2008).
33. Son, D. T. & Surówka, P. Hydrodynamics with triangle anomalies. *Phys. Rev. Lett.* **103**, 191601 (2009).
34. Lin, Q. & Fan, S. Light guiding by effective gauge field for photons. *Phys. Rev. X* **4**, 031031 (2014).
35. Fang, K., Yu, Z. & Fan, S. Realizing effective magnetic field for photons by controlling the phase of dynamic modulation. *Nat. Photon.* **6**, 782–787 (2012).
36. Zyuzin, V. A. Landau levels for an electromagnetic wave. *Phys. Rev. A* **96**, 043830 (2017).
37. Fradkin, E. Critical behavior of disordered degenerate semiconductors. ii. Spectrum and transport properties in mean-field theory. *Phys. Rev. B* **33**, 3263–3268 (1986).
38. Klier, J., Gornyi, I. V. & Mirlin, A. D. From weak to strong disorder in Weyl semimetals: self-consistent born approximation. *Phys. Rev. B* **100**, 125160 (2019).
39. Hulst, H. & van de Hulst, H. in *Dover Books on Physics*. https://books.google.com.br/books?id=PIHfPMVAFRcC (Dover Publications, 1981).
40. John, S. Localization of light. *Phys. Today* **44**, 32–40 (1991).
41. Lagendijk, A. & van Tiggelen, B. A. Resonant multiple scattering of light. *Phys. Rep.* **270**, 143–215 (1996).
42. Bialynicki-Birula, I. Photon wave function. *Prog. Optics* **36**, 245–294 (Elsevier, 1996).
43. Yamamoto, N. Photonic chiral vortical effect. *Phys. Rev. D.* **96**, 051902 (2017).
44. Lv, B. Q. et al. Observation of three-component fermions in the topological semimetal molybdenum phosphide. *Nature* **546**, 627–631 (2017).
45. Zhu, Y.-Q., Zhang, D.-W., Yan, H., Xing, D.-Y. & Zhu, S.-L. Emergent pseudospin-1 Maxwell Fermions with a threefold degeneracy in optical lattices. *Phys. Rev. A* **96**, 033634 (2017).
46. Efetov, K. B. *Supersymmetry in Disorder and Chaos* (Cambridge University Press, Cambridge, 1997).
47. Mirlin, A. D. Statistics of energy levels and eigenfunctions in disordered systems. *Phys. Rep.* **326**, 259–382 (2000).
48. Evers, F. & Mirlin, A. D. Anderson transitions. *Rev. Mod. Phys.* **80**, 1355–1417 (2008).
49. Redlich, A. N. Parity violation and gauge noninvariance of the effective gauge field action in three dimensions. *Phys. Rev. D.* **29**, 2366–2374 (1984).
50. Ryu, S., Schnyder, A. P., Furusaki, A. & Ludwig, A. W. W. Topological insulators and superconductors: tenfold way and dimensional hierarchy. *N. J. Phys.* **12**, 065010 (2010).
51. Schmidt, M. K. et al. Isotropically polarized speckle patterns. *Phys. Rev. Lett.* **114**, 113902 (2015).
52. Negoro, H., Sugimoto, H. & Fujii, M. Helicity-preserving optical metafluids. *Nano Lett.* **23**, 5101–5107 (2023).
53. MacKintosh, F. C., Zhu, J. X., Pine, D. J. & Weitz, D. A. Polarization memory of multiply scattered light. *Phys. Rev. B* **40**, 9342–9345 (1989).
54. Bicout, D., Brosseau, C., Martinez, A. S. & Schmitt, J. M. Depolarization of multiply scattered waves by spherical diffusers: Influence of the size parameter. *Phys. Rev. E* **49**, 1767–1770 (1994).
55. Gorodnichev, E. E., Kuzovlev, A. I. & Rogozkin, D. B. Depolarization of circularly polarized light in the Mie resonance region. *J. Phys. Conf. Ser.* **788**, 012039 (2017).
56. Altland, A. & Zirnbauer, M. R. Nonstandard symmetry classes in mesoscopic normal-superconducting hybrid structures. *Phys. Rev. B* **55**, 1142–1161 (1997).
57. Ryu, S., Schnyder, A. P., Furusaki, A. & Ludwig, A. W. W. Topological insulators and superconductors: tenfold way and dimensional hierarchy. *N. J. Phys.* **12**, 65010 (2010).
58. Wegner, F. The mobility edge problem: continuous symmetry and a conjecture. *Z. f.ür. Phys. B Condens. Matter* **35**, 207–210 (1979).
59. Altland, A., Simons, B. & Zirnbauer, M. Theories of low-energy quasi-particle states in disordered d-wave superconductors. *Phys. Rep.* **359**, 283–354 (2002).
60. Zirnbauer, M. R. Wegner model in high dimension: U(1) symmetry breaking and a non-standard phase of disordered electronic matter. I. One-replica theory. https://arxiv.org/abs/2309.17323 (2023).

Acknowledgements
We thank Antonio Zelaquett Khoury and Felipe Pinheiro for stimulating discussions and helpful comments on the manuscript. We acknowledge financial support from Brazilian agencies CNPq and FAPERJ and the Deutsche Forschungsgemeinschaft (DFG) project grant 277101999 within the CRC network TR 183 (subproject A03).

Author contributions
T.M. and A.A. contributed to the development of ideas, calculations, the discussion of results and the writing of the manuscript.

Funding
Open Access funding enabled and organized by Projekt DEAL.

Competing interests
The authors declare no competing interests.

Additional information
Supplementary information The online version contains supplementary material available at https://doi.org/10.1038/s42005-025-02191-1.

Correspondence and requests for materials should be addressed to Tobias Micklitz or Alexander Altland.

Peer review information *Communications Physics* thanks Fangwei Ye and the other, anonymous, reviewer(s) for their contribution to the peer review of this work. A peer review file is available.